EFFECT OF ALKALI TREATMENT ON THE TENSILE PROPERTIES OF GRAPE CANE FIBERS BY INTEGRATING DIGITAL IMAGE CORRELATION METHOD

*Balkis Fatomer A. Bakar**†*

Department of Natural Resource Industry
Faculty of Forestry and Environment
Universiti Putra Malaysia
Serdang 43000, Malaysia
and
Graduate Research Assistant
Wood Science and Engineering
College of Forestry
Oregon State University
Corvallis, OR 97330
E-mail: bfatomer@upm.edu.my

Frederick A. Kamke†

Professor
Wood Science and Engineering
College of Forestry
Oregon State University
Corvallis, OR 97330
E-mail: fred.kamke@oregonstate.edu

(Received April 2020)

Abstract. The objective of this study was to investigate tensile properties of two grape cane fibers, namely, outer bark (OB) and inner bark (IB). The cane is a necessary annual by-product from vineyards and is produced at approximately 36 million tons yearly around the world, which currently has no substantial commercial utilization. Grape cane fibers were subjected to an alkali treatment, at different concentrations, to separate the fibers from the cane. Moreover, two displacement methods such as system compliance (C_s) and digital image correlation (DIC) were performed to determine Young's modulus of the samples, and the results were compared. The OB fibers had better overall properties than IB fibers. The effect of the treatment concentrations (1, 3, 5, and 7 wt% of sodium hydroxide) and gage lengths (10, 25, and 40 mm) on the tensile properties was not consistent for both fiber types. The DIC method consistently yielded greater tensile modulus of the samples than the C_s method for OB fibers.

Keywords: Agricultural waste fibers, tensile test, digital image correlation, alkali treatment, grape cane fiber.

INTRODUCTION

Plant fibers have a broad range of tensile properties, and this variability depends on two main factors: fiber and precision measurement of the test equipment. The examples of the former factor are fiber separation process, treatment types, and the properties of the fiber itself, such as microfibril angle. Factors affecting the precision measurement include the grip system, crosshead speed, and the displacement measurement system. A wide-ranging variation of tensile properties, among and within plant varieties and fiber condition, has been reported, as shown in Table 1. For instance, a study to investigate the tensile properties of five different plant fibers, namely, curaua, sisal, jute, piassava, and coir, was conducted by Alves Fidelis et al (2013). They categorized the first three fibers as higher performance fibers because the tensile

* Corresponding author
† SWST member

Wood and Fiber Science, 52(4), 2020, pp. 365-379
https://doi.org/10.22382/wfs-2020-035

Table 1. Mean values and standard deviations of single fiber tensile properties of previously reported plant fibers.

Fiber	Fiber condition	Tensile strength (MPa)	Young's modulus (GPa)	Reference
Hemp	5% NaOH	911.3 ± 315.6	26.4 ± 13.3	Aruan Efendy and Pickering (2014)
Hemp	Heat treatment	244 ± 196	8.6 ± 5.9	Shahzad (2013)
Jute	Retting	249 ± 89	43.9 ± 12.3	Alves Fidelis et al (2013)
Abaca	5% NaOH	773 ± 119	25.3 ± 6.3	Cai et al (2016)
Harakeke	5% NaOH	641.3 ± 209.6	20.8 ± 8.6	Aruan Efendy and Pickering (2014)
Date palm fiber	6% NaOH	366 ± 36.4	5.45 ± 1.4	Abdal-hay et al (2012)
Cotton stalk	Decortication	510	13.2	Yzombard et al (2014)
Curaua	Decortication	543 ± 260	63.7 ± 32.5	Alves Fidelis et al (2013)
Coir	Retting and decortication	90 ± 35	2.6 ± 0.7	Alves Fidelis et al (2013)
Coir (brown)	Mechanically extracted	165-222	3.79	Biswas et al (2013)

NaOH, sodium hydroxide.

strength was above 249 MPa. Meanwhile, the remaining fibers were classified as low-performance fibers and had tensile strength below 131 MPa.

One of the factors contributing to the variability of the tensile properties is difficulty in measuring the cross-sectional area. Generally, technical fibers have a nonuniform cross section and irregular shape along the fiber length. The area used in the tensile property calculation is based on the projected outer diameter of the fiber, assuming a cylindrical shape, and the lumen is neglected (Shah et al 2017). Several methods for calculating the cross-sectional area of the fibers have been reported. For example, averaging the fiber diameter or width along the fiber length using an optical microscope (Ilankeeran et al 2012; Biswas et al 2013; Shahzad 2013; Fiore et al 2016), using SEM to measure the contour of the fiber cross-sectional area (Silva et al 2008), and by considering the mass and density of the fibers (Defoirdt et al 2010; Depuydt et al 2017). Despite having numerous studies, several authors did not include the required information for the simplicity of comparison.

Using an extensometer to measure the elongation during the test for measuring Young's modulus is not possible because a technical fiber has a very small diameter, with a range of 119-800 μm (Abdal-hay et al 2012; Cai et al 2016; Fiore et al 2016). In addition, the placement of the extensometer on the fiber interferes with the fiber's response to the applied force. Therefore, the displacement is often measured indirectly by using the crosshead movement and incorporating system compliance (C_s) correction (ASTM C1557-14 2014). The tensile test needs to be carried out at three different gage lengths of the same material to use the C_s correction. Therefore, it requires a significant amount of test material and is time consuming and not convenient when it is desired (Depuydt et al 2017).

Moreover, the accuracy of the displacement measurement of fibers is reported to contribute to the variability of the measured value of tensile properties, and it has not been generally addressed (Depuydt et al 2017). Digital image correlation (DIC) has been reported to be widely used to measure displacements and strain heterogeneity in a material during mechanical tests (Depuydt et al 2017; Schwarzkopf et al 2017; Cerbu et al 2018; Burnard et al 2019). Moreover, integrating the DIC method has been reported to have more benefit than the conventional strain measurement, especially in a composite material (Zhao and Zhao 2013; Ab Ghani 2016).

Grape cane is generated from vineyards at an annual rate of approximately two oven-dry tons per acre, with the majority incinerated. There are about 18 million acres of vineyard around the world (Wine Institute 2014; Toscano et al 2018), and it has been observed that there is an increasing trend to explore the potential of grape cane materials in various applications (Alma and Basturk 2006; Mancera et al 2011; Yeniocak et al 2014). The main objective of this study was to characterize tensile properties of alkali-treated grape cane fibers measured by two different displacement methods. The effect of gage lengths

on the measured values of tensile properties and the comparison between methods of measuring the fiber elongation during the test to determine Young's modulus were reported. In addition, these fibers were subjected to different concentrations of sodium hydroxide (NaOH) solution to improve the fiber surface by removing the impurities on the fibers.

MATERIALS AND METHODS

Grape Cane Fibers and Fiber Treatment

Grape canes were obtained in February from a local vineyard located in the Willamette Valley region of Oregon in the United States. The cane fibers can be categorized into two types: outer bark (OB) and inner bark (IB) based on their location across the transverse section of the cane. The OB fiber is extracted from the outermost layer of the cane, which is also called a periderm layer. Meanwhile, the IB fiber is extracted from the secondary phloem, which is located on the outer side of the vascular cambium in the cane. These fibers have similar chemical compositions and fiber morphology like other plant fibers.

Alkali treatment is carried out to separate these fibers from the cane and to improve the hydrophilicity and topography of the fibers following Bakar and Kamke (2020). Four concentrations of NaOH were used to investigate the effects of the treatment concentrations on the fiber properties. They are labeled as N1, N3, N5, and N7 representing 1, 3, 5, and 7 wt% NaOH. These fibers (OB and IB fibers) were treated individually to examine their tensile properties separately. Figure 1 shows these fibers have different textures; OB fibers were coarser and thicker than IB fibers.

Tensile Test Setup and Specimen Preparation

The tensile test of the samples was carried out on an Instron ElectroPuls E1000 (Instron, Norwood,

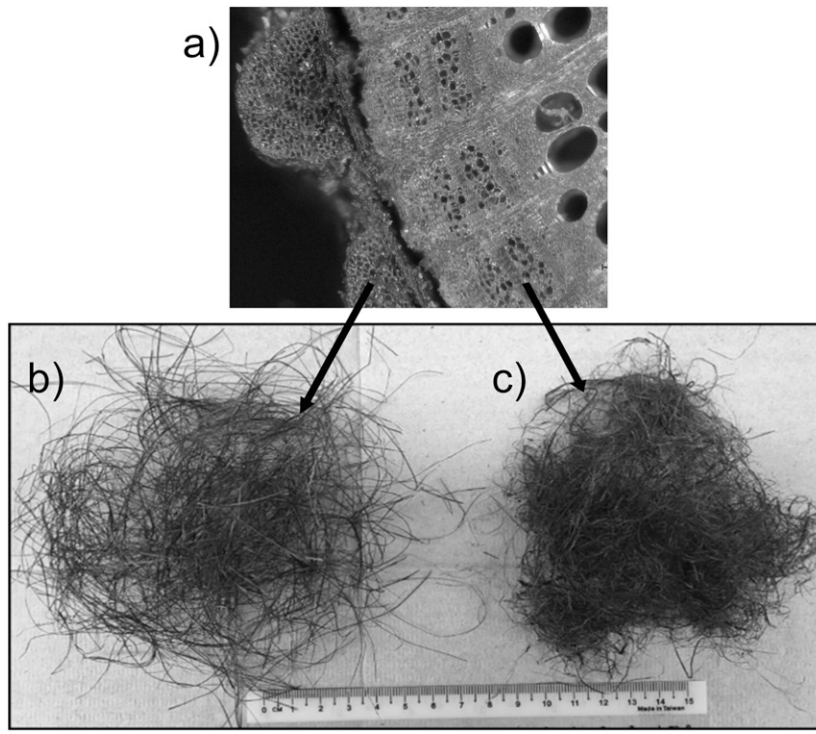

Figure 1. (a) Cross section of grape cane, (b) treated outer bark fibers, and (c) treated inner bark fibers.

MA) universal testing machine (UTM) according to ASTM C1557-14 (2014); 100 N and 5 N load cell capacities were installed onto the UTM for the OB and IB fibers, respectively, and the crosshead speed of 2 mm/min was used for the test (ASTM C1557-14 2014). A single technical fiber from each treatment was mounted on a paper frame, and two speckle pattern targets were glued at both ends of the fiber (Fig 2). Test specimens were conditioned at a temperature of 20°C and 65% RH for 24 h before the testing. The paper frame was held by the UTM grips reinforced with sandpaper to reduce the slippage effect.

Indirect Displacement Measurement: ASTM C1557-14

Fiber elongation during the tensile test can be calculated using the crosshead displacement of the UTM with a crosshead movement precision of $\pm 1^{-03}$ mm. According to the ASTM C1557, the actual fiber elongation can be measured by considering the C_s. The C_s is defined as any movement from the load train system and specimen-gripping system during the test that contributes to the total crosshead movement. Therefore, the total crosshead displacement can be calculated as given in Eq 1.

$$\Delta L = \Delta l + C_s \Delta F, \tag{1}$$

where ΔL is the recorded crosshead displacement, Δl is the elongation of the specimen gage length, C_s is the system compliance, and F is the applied force.

Three gage lengths were used in the current study: 10, 25, and 40 mm and were labeled as G10, G25, and G40, respectively. For each test specimen at each gage length, the inverse of the slope of the initial linear region of the force vs crosshead displacement ($\Delta L/F$) curve was obtained. Combining Hooke's law (Eq 2) and fiber strain equation (Eq 3) to Eq 1 resulted in the C_s as the intercept value of a plot of $\Delta L/\Delta F$ vs l_o/A (Eq 4).

$$\Delta \varepsilon = \frac{\Delta \sigma}{E} = \frac{\Delta F}{AE}, \tag{2}$$

$$\Delta \varepsilon = \frac{\Delta l}{l_o}, \tag{3}$$

$$\frac{\Delta L}{\Delta F} = \frac{\Delta l}{\Delta F} + \quad C_s = \frac{l_o}{AE} + C_s, \tag{4}$$

where $\Delta\varepsilon$ is the tensile strain change from the prestress level, $\Delta\sigma$ is the tensile stress change from the prestress level, E is fiber Young's modulus, l_o is gage length, and A is fiber cross-sectional area. Therefore, the actual fiber elongation can be calculated based on Eq 5 for each combination of gage length and fiber type. A total of 480 test specimens were conducted for this test.

$$\Delta l = \Delta L - C_s F \tag{5}$$

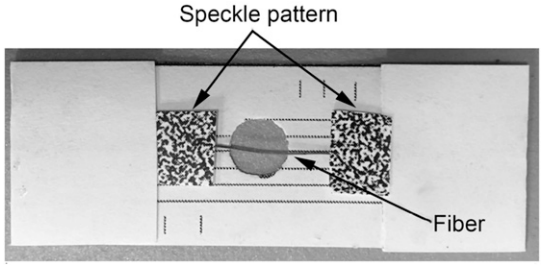

Figure 2. Example of a tensile test specimen following ASTM C1557 with speckle pattern targets.

Direct Displacement Measurement: DIC Method

A DIC system detects motion of an object by comparing two images, of the same field of view, of unique patterns of digital image data on the surface of the object. This system detects motion by correlating subsets of the speckle pattern between the two images and a known, spatially calibrated, coordinate system. Therefore, the reliability of the results relies on two elements: the quality of the speckle pattern and the camera resolution (Ab Ghani 2016; Schwarzkopf et al 2017).

The speckle patterns should be random in size and distribution, as well as have good contrast between the patterns and the sample background (Fig 2). These speckle pattern targets were

generated by considering the randomization of the dot size and distribution suitable for the size of the test specimen and field of view and was laser printed on a white paper. Before testing, these speckle pattern targets were mounted on the paper frame and tested for repeatability. Without applying a load, a sequence of six images were captured and analyzed for any significant movements to validate for background noise. The standard deviation of the background noise or the precision of the optical measurement for horizontal and vertical directions was $\pm 2.42^{-04}$ and $\pm 1.51^{-04}$ mm, respectively.

Figure 3 shows the DIC experimental setup of the tensile test. Two cameras (Point Grey, FLIR Systems, Inc., Wilsonville, OR), with a maximum resolution of 2,448 × 2,048 pixels, and lens 1.9/35 (Xenoplan, Schneider Kreuznach, Hauppauge, NY) were used. The distance between the cameras and the specimen was approximately 35 cm, and the captured image had a square pixel of 0.0192 mm. The camera setup and lens distortion were calibrated using a 1-in. calibration target grid with 91 calibration dots provided by the manufacturer (Correlated Solutions, Columbia, SC) for each gage length setup. A sequence of images was taken during the test at 100-ms intervals until the specimen failed.

All captured DIC method images were analyzed using VIC-3D analytical software (Correlated Solutions) based on the area of interest (AOI). This AOI was selected on the speckle pattern targets and was used to analyze the fiber displacement. A subset size and a step size were set at 49 and 7 pixels, respectively. Fiber elongation data were extracted by using a virtual extensometer tool in postprocessing software. The tool analyzes the movement along a line parallel to the fiber to indicate the elongation of the fiber in the axial direction and is used to calculate the tensile modulus.

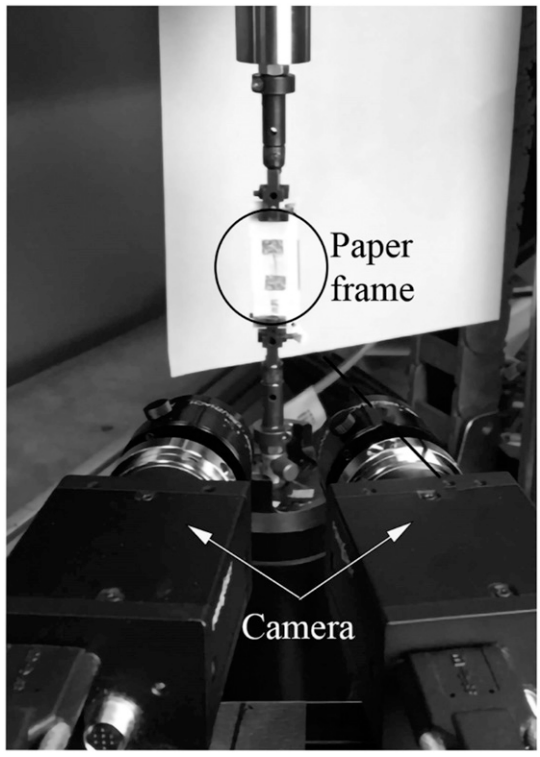

Figure 3. Tensile test setup integrated with the digital image correlation system.

Fiber Morphology Using SEM

The untreated and treated fibers were examined using an FEI QUANTA 600F (Thermo Fisher Scientific, Hillsboro, OR) environmental SEM. Two technical fibers were mounted parallel and perpendicular to the aluminum stubs and secured with carbon tape. The parallel fibers were prepared to observe the effect of the treatment concentrations on the fiber surface. Perpendicular fibers were prepared after soaking about 30 s in liquid nitrogen and then fractured to observe the shape of the cross section of the fibers. In addition, measurements of the cross-sectional area of these fibers were recorded. The fibers were handled with care to ensure no pressure was applied on the fibers to avoid external defects. The mounted samples were then sputter-coated with gold/palladium for 35 s. A high vacuum voltage of 5 kV and magnification of 130× to 1,000× (field of view 1.97-256 μm) were applied during image capture.

Statistics Analysis

The data were statistically analyzed using R studio software, version 1.2.1335 (R studio,

Boston, MA). Analysis of variance (ANOVA) was used to examine the effects of treatment concentrations and gage lengths on the tensile properties of grape cane fibers. The analysis was performed separately for OB and IB fibers because of the substantial difference in the tensile properties to satisfy the ANOVA assumptions. Tukey's honest significant difference (Tukey HSD) test was used for further evaluation on the effect of the main parameter on each tensile property tested. The Tukey HSD test ranks the means and calculates the minimum value to be significantly different from each other at $p < 0.05$. Means followed by the same letter a, b, c, etc. are not significantly different. An additional symbol after the letter may indicate that the tensile properties were analyzed separately based on a specific parameter that will be mentioned in that particular section.

RESULTS AND DISCUSSION

Tensile Behavior of Grape Cane Fibers

Figure 4 shows a stress–strain curve of OB and IB fibers that were subjected to the same condition, where both fibers were treated with N1 treatment and tested at G25. Both fibers exhibited brittle material properties when the fibers failed abruptly without any noticeable change in the elongation rate. The OB fibers have higher tensile strength and Young's modulus and lower strain to failure (DIC method) than IB fibers.

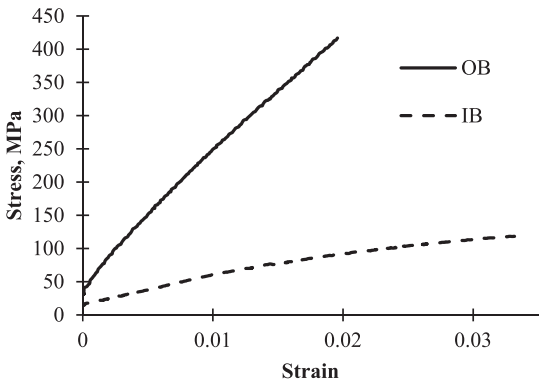

Figure 4. Comparison stress–strain curve between outer bark and inner bark fibers using the digital image correlation displacement method.

These fibers can further be divided into two groups: high- and low-performance fibers based on tensile strength (Alves Fidelis et al 2013). Based on the following article's criteria, grape cane OB fibers can be classified as high-performance fibers, whereas IB fibers are low-performance fibers. The difference in the tensile properties of these fibers may be due to the makeup of the technical fiber. OB and IB fibers are made up of different cell types that have different functions in living trees and the cross section of the fibers after the treatment process showing they have distinctive cross-sectional shapes and structures (Bakar and Kamke 2020).

The OB fibers, also known as periderm, is the outermost layer of the bark and functions as a protection layer from abiotic and biotic agents. The fibers are made up of cork cells (Pereira 2007), which is in contrast to the IB fibers that are made up mostly of sclerenchyma cells. The IB fibers originated from the secondary phloem, which is the outer layer after the thin layer of the vascular cambium of the grape cane. The function of IB fibers, in general, is to transport nutrients, and sclerenchyma cells are more as a support system in a living tree because of its thick cell wall. The differences in the fiber origin and morphology contribute to the distinctive tensile behaviors.

Tensile Properties of Grape Cane Fibers

Table 2 summarizes the mean value of parameters tested for OB fibers. Lower treatment concentrations, N1 and N3, resulted in higher tensile properties than the higher treatment concentrations. However, the strain at failure values had inconsistent treatment effects. The gage length effect statistically indicated that G10 resulted in the lowest tensile properties of OB fibers but had the highest strain at failure.

Similar to OB fibers, lower treatment concentrations produced fibers with higher tensile properties (Table 3). Meanwhile, the effect of gage length was inconsistent for tensile strength and tensile modulus. For instance, IB fibers tested

Table 2. Mean values of the effect from gage lengths and treatment concentrations on tensile strength, tensile modulus, and strain to failure for outer bark grape cane fibers using digital image correlation method.

Gage length	Treatment	Tensile strength (MPa)	Tensile modulus (GPa)	Strain at failure (%)
G10	N1	305.6^{a} (97.5)	9.4^{ab} (4.5)	3.6^{a} (1.8)
	N3	339.2^{a} (74.0)	11.0^{a} (3.2)	2.9^{b} (0.8)
	N5	286.8^{a} (84.2)	7.2^{bc} (2.5)	3.6^{a} (1.0)
	N7	199.0^{b} (108.1)	4.8^{c} (4.5)	3.9^{a} (0.6)
G25	N1	$388.3^{a'}$ (108.1)	$15.8^{a'}$ (4.5)	$2.1^{c'}$ (0.6)
	N3	$395.6^{a'}$ (123.2)	$14.5^{a'}$ (4.0)	$2.3^{bc'}$ (0.6)
	N5	$291.9^{b'}$ (110.0)	$8.3^{b'}$ (1.8)	$3.2^{a'}$ (0.6)
	N7	$276.9^{b'}$ (83.4)	$8.7^{b'}$ (2.7)	$2.8^{ab'}$ (0.7)
G40	N1	$404.0^{a''}$ (78.7)	$13.0^{a''}$ (2.9)	$2.9^{a''}$ (0.8)
	N3	$374.5^{ab''}$ (113.9)	$11.6^{a''}$ (3.2)	$2.7^{a''}$ (0.7)
	N5	$305.6^{bc''}$ (87.5)	$8.1^{b''}$ (1.4)	$2.9^{b''}$ (0.7)
	N7	$239.8^{b''}$ (67.5)	$7.1^{b''}$ (1.9)	$2.7^{b''}$ (0.4)

Data are expressed as mean and SD (within parentheses) based on 17 measurements. Means followed by the same superscripted letter(s) in the same column are not significantly different at $p \leq 0.05$. An additional symbol after the letters indicates separate analysis was performed for each gage length.

at G10 had the highest mean value of tensile strength but the lowest for the tensile moduli.

Of all tensile properties, OB fibers consistently resulted in higher properties than IB fibers, regardless of the treatment concentration and gage length effects. Differences in fiber morphology greatly influenced the fiber properties as discussed earlier.

Tensile Strength of Grape Cane Fibers

Treatment concentration effect. Figure 5 presents stress–strain curves for individual OB and IB fibers according to the treatment concentrations. Regardless of the treatment concentrations, the IB fibers were less brittle and more ductile (Fig 5[b]) than OB fibers. There was no apparent strain to failure fluctuations observed for IB fibers.

Increasing treatment concentrations reduced the tensile strength and increased the strain to failure, except for N7 treatment of the OB fibers (Fig 5[a]). For all gage lengths, fibers treated with N1 and N3 treatments resulted in higher tensile strength with an overall mean value of 366.0 and 369.7 MPa, respectively. Meanwhile, at N5 and N7 treatments, the fibers had 294.8 and 238.6 MPa, respectively. A similar trend to the tensile strength was observed for the tensile moduli of

Table 3. Mean values of the effect from gage lengths and treatment concentrations on tensile strength, tensile modulus, and strain to failure for inner bark grape cane fibers using digital image correlation method.

Gage length	Treatment	Tensile strength (MPa)	Tensile modulus (GPa)	Strain at failure (%)
G10	N1	162.8^{b} (41.97)	2.0^{b} (0.79)	5.3^{ab} (1.9)
	N3	323.2^{a} (74.95)	2.9^{a} (1.09)	7.5^{ab} (3.4)
	N5	154.4^{b} (40.75)	0.9^{c} (0.26)	9.3^{a} (3.3)
	N7	104.4^{c} (17.14)	0.8^{c} (0.25)	6.9^{b} (2.7)
G25	N1	$130.5^{b'}$ (39.75)	$3.5^{a'}$ (1.2)	$3.2^{a'}$ (1.2)
	N3	$209.6^{a'}$ (57.20)	$2.3^{b'}$ (1.2)	$3.7^{a'}$ (1.5)
	N5	$101.2^{bc'}$ (28.72)	$2.3^{b'}$ (0.9)	$3.8^{a''}$ (1.5)
	N7	$84.6^{c'}$ (23.25)	$1.1^{c'}$ (0.5)	$3.2^{a'}$ (1.2)
G40	N1	$136.2^{b''}$ (41.75)	$2.8^{a''}$ (0.7)	$2.8^{b''}$ (1.6)
	N3	$207.9^{a''}$ (58.38)	$4.4^{b''}$ (1.3)	$3.3^{a''}$ (1.7)
	N5	$94.6^{c''}$ (24.72)	$1.9^{c''}$ (0.5)	$3.3^{c''}$ (1.6)
	N7	$84.0^{c''}$ (22.98)	$1.3^{c''}$ (0.4)	$4.1^{c''}$ (1.6)

Data are expressed as mean and SD (within the parentheses) based on 17 measurements. Means followed by the same superscripted letter(s) in the same column are not significantly different at $p \leq 0.05$. An additional symbol after the letters indicates separate analysis was performed for each gage length.

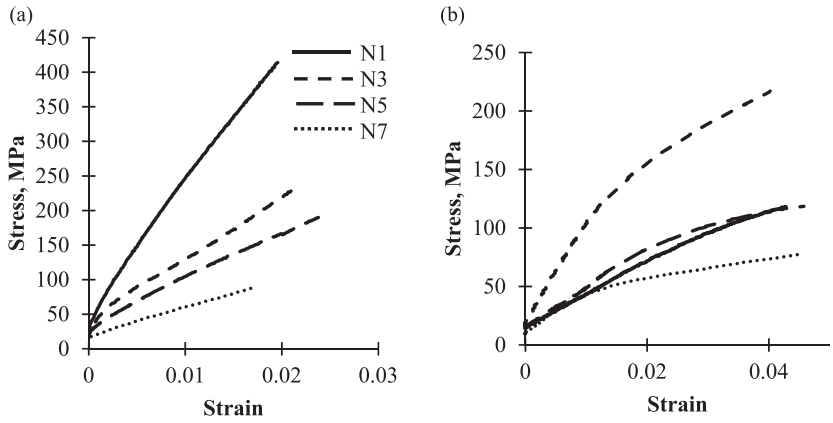

Figure 5. Stress–strain curve between treatment concentrations for (a) outer bark fibers and (b) inner bark fibers using the digital image correlation method.

OB fibers with mean values of 12.8, 12.3, 7.9, and 6.9 GPa with increasing treatment concentrations.

In contrast to the OB fibers, tensile strength of the IB fibers treated in N3 was significantly greater than that in other treatment concentrations with a mean value of 246.9 MPa. Meanwhile, fibers treated in N7 had the lowest tensile strength with 91.0 MPa. A similar treatment concentration effect to tensile strength was observed for tensile modulus. Fibers treated with N1 and N3 had the highest moduli with mean values of 2.8 and 3.2 GPa, whereas the lowest values were found for N5 and N7 treatments with 1.7 and 1.0 GPa, respectively.

The overall mean of tensile strength was 317.3 and 149.4 MPa for OB and IB fibers, respectively, for all treatment and gage length effects. A pronounced difference of tensile properties between OB and IB fibers is attributed to the different fiber morphological shapes (Bakar and Kamke 2020). Because of different fiber morphologies, the effect of the alkali treatment on the fibers was different. The IB fibers were more susceptible to the NaOH treatment and, consequently, had more fibrillation at higher treatment concentration as shown in Fig 6. Potentially weak points occurred on the fibers because of fibrillation, which eventually reduced the force required to fail the specimen (Cai et al 2016; Oushabi et al 2017). In addition, higher crystallinity index of the technical fibers and aspect ratio of the morphological unit will provide the strength to the OB fibers (Bakar and Kamke 2020).

At higher treatment concentrations, more binder substances, such as lignin and pectin in the cell wall and in the middle lamella that connect single fibers together in a bundle, as well as other amorphous materials on the fiber surfaces, were dissolved into the treatment solution. Therefore, it is important to determine the optimum treatment concentration to avoid excessive fibrillation or insufficient active ingredient of the treatment to remove the impurities based on the fiber types. The results from this study showed that both grape cane fibers had better tensile properties when they were treated at lower treatment concentrations (N1 and N3).

Gage length effect. Table 4 presents the mean values for tensile strength and tensile modulus

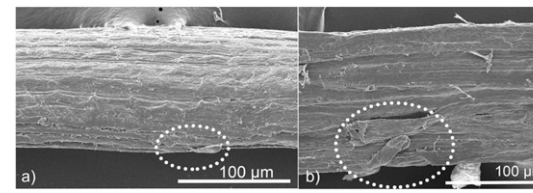

Figure 6. SEM micrographs of grape cane fiber surface after N7 treatment at 1,000× magnification, (a) outer bark fiber and (b) inner bark fiber. Dashed circle presents some of the defibrillation spots.

Table 4. Mean values of the effect from gage lengths on tensile strength and tensile modulus for OB and IB grape cane fibers using the digital image correlation method.

Fiber type	Gage length	Tensile strength (MPa)	Tensile modulus (GPa)
OB	G10	282.6^{b} (77.9)	8.1^{c} (3.1)
	G25	338.2^{a} (106.2)	11.9^{a} (3.2)
	G40	331.1^{a} (86.9)	9.9^{b} (2.3)
IB	G10	$186.2^{a'}$ (43.7)	$1.6^{b'}$ (0.6)
	G25	$131.5^{b'}$ (37.2)	$2.3^{a'}$ (1.0)
	G40	$130.7^{b'}$ (37.0)	$2.6^{a'}$ (0.7)

IB, inner bark; OB, outer bark. Data are expressed as mean and SD (within the parentheses) based on 68 measurements. Means followed by the same superscripted letter(s) in the same column are not significantly different at $p \leq 0.05$. An additional symbol after the letters indicates separate analysis was performed for each gage length.

based on the DIC method for each fiber type based on the gage length. The influence of gage length on the measured value of tensile strength was found to be contradictory between these two fibers. Fibers tested at G25 show the highest tensile strength and modulus for OB fibers; however, there is inconsistent trend observed for IB fibers.

The highest tensile strength for OB fibers was at G25 which may be due to the shorter fiber length does not carry the maximum load during the test. The increasing trend of the tensile properties of OB fibers with the gage length, to a certain extent, is in agreement with past studies that used coconut and *Phoenix* sp. fibers (Rajeshkumar et al 2016; Valášek et al 2017). Meanwhile, the highest tensile strength at the shortest gage length for IB fibers is similar to findings from past studies (Alves Fidelis et al 2013; Biswas et al 2013; Zeng et al 2015). They have reported that the strength is gradually reduced with increasing gage length; however, no statistical difference was found.

Longer technical fibers have been reported to have more weak linkages (flaws) within the single fibers in the fiber bundle as well as between the ultimate fibers in the single fibers, along the fiber length (Tomczak et al 2007; Defoirdt et al 2010; Biswas et al 2013). Biswas et al (2013) added these weak linkages reduce the load required to break the fiber. This explanation is consistent with the observations from the IB fibers in the current study. An additional analysis of width variation of a single technical fiber for each fiber type and treatment concentration was observed under an SEM (Fig 7). Three micrographs were taken for each combination of parameters.

The variation of fiber width taken at five points at the same interval along the fibers is given in Table 5. A mean value of five individual fibers for each combination of treatment concentration and fiber type was calculated. In general, the OB fibers have a lower width variation along the fiber length than IB fibers. Based on Bakar and Kamke (2020), OB fibers were assumed to have a circular cross section; meanwhile, IB fibers have a rectangular cross section. Therefore, the largest dimension was recorded as the IB fiber width as given in Table 5. The range of width deviation of OB and IB fibers was found to be 0.003-0.01 mm and 0.005-0.023 mm, respectively.

Consistency in the fiber width along the fiber length may be benefited to the stress transfer efficiencies along the fiber. Having a relatively less variation of fiber width may reduce the number of weak points that will be potentially the failure points. When force is applied, it distributes uniformly along the fibers, and ultimately, the fiber can withstand higher load before it fails. However, the fiber would break at the weakest linkage, and it does not necessarily fail at the smallest width (Martin et al 2013). Thus, having less variance of fiber width along OB fiber length

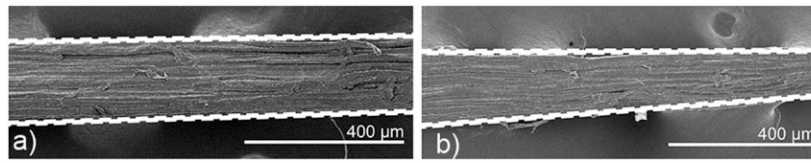

Figure 7. SEM micrographs of grape cane fibers at 250× magnification, (a) outer bark fiber and (b) inner bark fiber width. Note: Dotted lines show the approximation of fiber borderline.

Table 5. Overall means and standard deviations (within the parentheses) of grape cane fiber width corresponding to the treatment concentrations.

Treatment	Outer bark fiber (mm)	Inner bark fiber (mm)
N1	0.27 (0.010)	0.10 (0.016)
N3	0.13 (0.007)	0.06 (0.005)
N5	0.20 (0.006)	0.12 (0.023)
N7	0.11 (0.003)	0.15 (0.019)

contributes to more uniformity in terms of load transfer.

Comparison of Displacement Measurement Methods

Two displacement methods were compared to determine the tensile modulus of grape cane fibers and were tagged as C_s and DIC methods. Table 6 shows the C_s values varied for each fiber type and treatment concentration determined based on Eqs 1-4. In addition, the percentage of difference in the modulus derived from the DIC and C_s methods is presented in Table 6. Only OB fibers had statistical difference in tensile moduli when comparing these two methods (p-value is $1.608e^{-08}$). The overall mean for the modulus calculated based on the DIC method was found to be approximately 27.1% higher than C_s method for OB fibers. The calculated difference between these two methods may mainly be contributed to the slippage effect during the tensile test. This slippage effect was observed to be more apparent for stiffer fibers because higher load may produce more slippage between the specimen frame with the grip on the UTM or between the fibers and the specimen frame (Table 6 and Fig 9).

Figure 8 demonstrates an example of a post-processing analysis for a single fiber tensile test. Figure 8(a)-(c) present photos taken before, during, and after the tensile test. The colored contour in the AOI of the speckle pattern targets signifies the axial movement of the fiber during the test. Figure 8(d) displays the color contour scale for the axial displacement (vertical direction) of the fiber in millimeter unit. The left side of the range indicates no movement (0 value), and the right side represents the highest movement in the axial direction.

For simplicity, the modulus of OB and IB fibers tested at G25 according to the treatment concentrations were used as an illustration and presented in Fig 9(a) and (b), respectively. It was found that the DIC method produced higher modulus than C_s method by 31.6%, 23.6%, 18.5%, and 15.4% for OB fibers. By contrast, C_s method resulted in higher modulus than the DIC method for IB fibers, except for N1 treatment.

Increasing treatment concentrations showed less difference in the modulus between these methods, similar to other gage lengths (Fig 10). This finding supports the idea that higher load required to break the specimen has more slippage effect (Zhao and Zhao 2013; Ab Ghani 2016; Depuydt et al 2017). Moreover, longer gage lengths have a lower difference in the modulus between these two methods. For instance, the difference in the modulus between these two methods for OB-N1 fibers tested at G10, G25, and G40 was 44%,

Table 6. System compliance and difference percentage between the DIC and C_s methods corresponding to the fiber types and treatment concentrations.

Fiber type	Treatment	System compliance value	Differences between DIC and C_s methods (%)
Outer bark	N1	0.011	41.7
	N3	0.014	25.6
	N5	0.015	22.9
	N7	0.012	12.2
Inner bark	N1	0.073	9.0
	N3	0.408	(7.7)
	N5	0.943	(3.5)
	N7	0.578	(12.9)

Data given within parentheses indicate the C_s method had higher values than the DIC method.

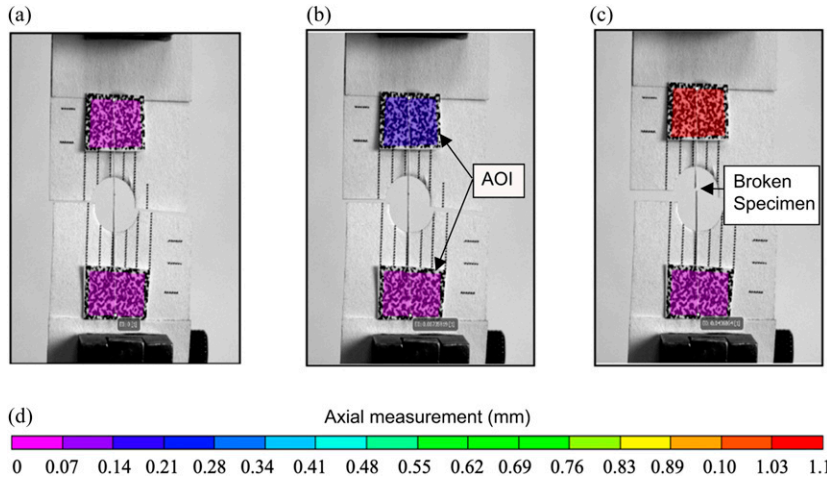

Figure 8. Photos taken (a) before, (b) during, (c) after tensile test, and (d) the axial movement representation of fiber elongation.

31%, and 13%, respectively. This finding is consistent with a past study that investigated jute, bamboo, brown coir, and white coir fibers (Biswas et al 2013). They observed longer gage lengths had a smaller relative effect of slippage in the clamps to the measured machine displacement.

Less difference between the modulus, due to the displacement measurement method, was found for IB fibers compared with OB fibers. This is simply due to the fact that the IB fibers had a very low failure load and, hence, less slippage in the grips. The C_s method system assumed that the material tested is homogenous along the fiber length. Unlike a synthetic fiber, where the manufacturing properties can be controlled and can be relatively homogenous, a single bundle of technical plant fiber is made up of several elementary fibers that are formed from ultimate fibers (Bakar and Kamke 2020). Because of these interconnecting elementary fibers to make up one test specimen, plant fibers have numerous irregularities along their length, and the probability of a critical flaw increases with gage length. Moreover, the C_s system measures the elongation of the whole test setup (including the

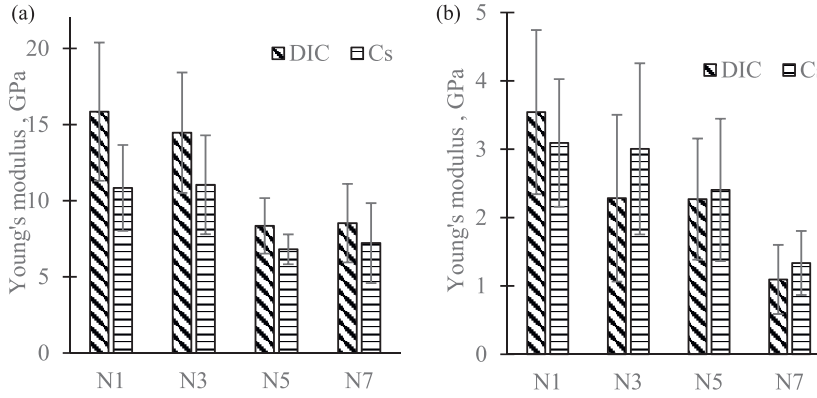

Figure 9. Young's modulus of grape cane fibers using the DIC and C_s methods for (a) outer bark and (b) inner bark corresponding to the treatment concentration at 25 mm gage length.

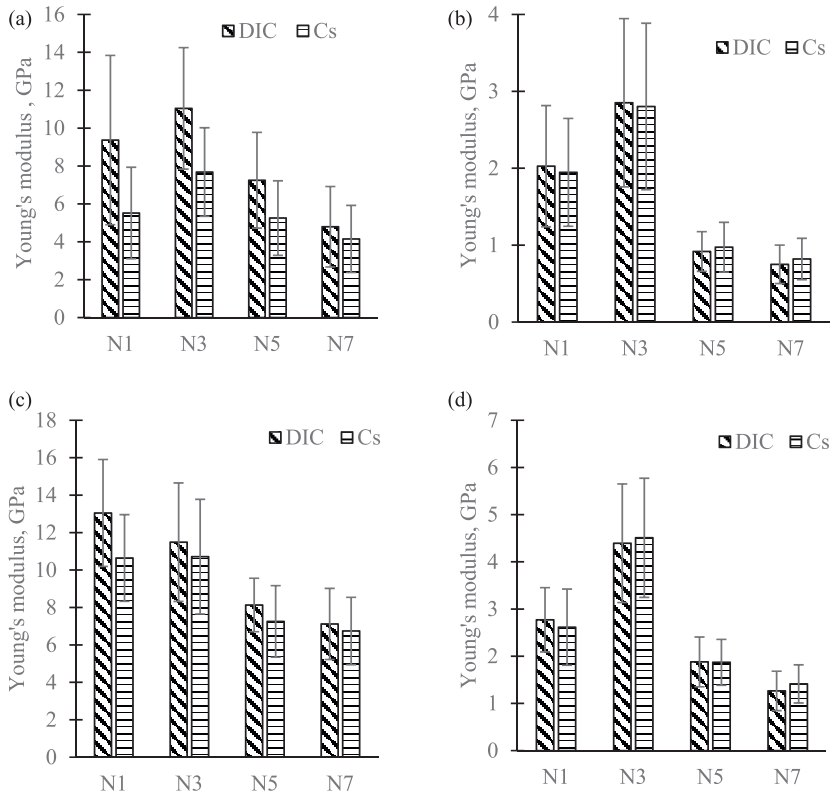

Figure 10. Young's modulus of grape cane fibers using the DIC and C_s methods at gage length 10 mm for (a) outer bark (OB) and (b) inner bark (IB), and at gage length 40 mm for (c) OB and (d) IB corresponding to the treatment concentrations.

paper frame and grip system, as well as a test specimen with the paper frame), which contributes to the slippage effect that was observed in this study. By contrast, the DIC method system visually focuses on the elongation of the fibers during the test independent of the grips and test frame. Therefore, the modulus calculated based on the DIC method will be used henceforward.

Tensile Modulus of Grape Cane Fibers

The effect of treatment concentrations and gage lengths on the tensile modulus was observed for OB (Fig 11[a]) and IB fibers (Fig 11[b]) based on the DIC method. In general, OB fibers have a 4-fold higher modulus than IB fibers. Increasing treatment concentrations have revealed two distinct groups: higher and lower moduli for OB fibers. The higher group consists of fibers treated in N1 and N3 treatment concentrations, whereas N5 and N7 treatments in the lower group, regardless of the fiber types. There were inconsistent gage length effects for IB fibers based on the treatment concentrations.

The tensile modulus is dependent on several factors, such as fiber crystallinity, cellulose content, cell wall thickness, fiber diameter, size of the lumen, and defects (Tomczak et al 2007; Placet et al 2012; Huang and Fei 2017; Goudenhooft et al 2018; Zhang et al 2019). For example, the OB fibers treated with N1 and N3 treatment concentrations have higher crystallinity index with 61.0% and 60.2%, respectively. Lower crystallinity index was found for N5- and N7-treated fibers, which were 55.0% and 56.8%, respectively. These results from Bakar and Kamke (2020) support the finding of the

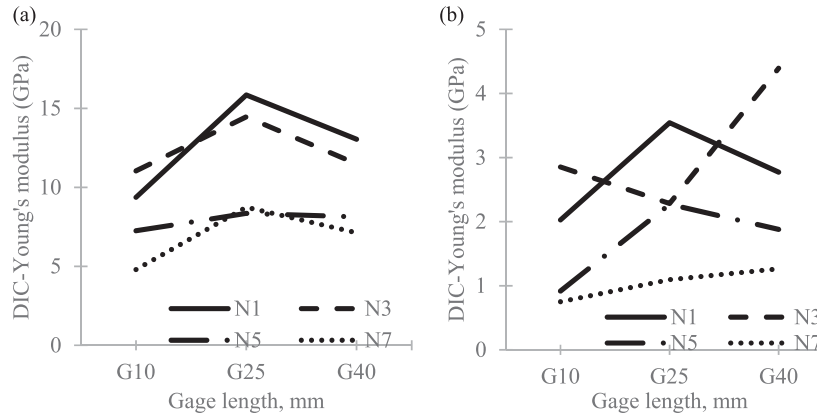

Figure 11. Young's modulus calculated based on the digital image correlation method for (a) outer bark fibers and (b) inner bark fibers according to treatment concentrations at different gage lengths.

current study. Furthermore, the crystallinity of IB fibers treated in N1 treatment concentration was 45.4%, which is lower than that of OB fibers (Bakar and Kamke 2020). IB fibers were observed to have thinner cell wall with a mean value of 1.3 μm than OB fibers (3.4 μm) as shown in Fig 12. In addition, high width variability along the fiber length (Fig 7) of IB fibers may contribute to a higher number of weak points and less efficiency to transfer load during the test, leading to less resistance to the elastic deformation. The segmented cell wall of IB fibers, which is believed to be pits, was observed to be more apparent after alkali treatment (Bakar and Kamke 2020). This feature can contribute to lowering the fiber strength of IB fibers because pits are said to be natural fiber defects and the stress concentrations often occur at or around the pit location when subjected to the tensile test (Huang and Fei 2017).

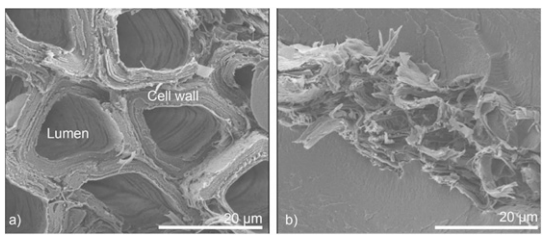

Figure 12. SEM micrographs of the cross section of (a) outer bark fiber and (b) inner bark fiber at 500× magnification.

CONCLUSIONS

Tensile properties of two fiber types extracted from grape cane were determined according to the treatment concentrations and gage lengths. Overall, the OB fibers were found to have higher tensile strength and Young's modulus by at least four times than IB fibers. The DIC method consistently yielded a greater tensile modulus than the C_s method for OB fibers compared with IB fibers.

Treatment concentrations had less significant influence on IB fibers than OB fibers. However, fibers treated at the lower concentrations, which were N1 and N3, had higher tensile properties. Meanwhile, N7 treatment produced the lowest tensile properties, regardless of the fiber types. The optimum gage length found in the current study for both fibers was 25 mm for OB fibers, whereas there was inconsistency found in IB fibers. The irregularity of IB fiber width along the fiber length, thinner cell wall thickness, lower cellulose content, and crystallinity may have contributed to this cause.

Based on the results, OB fibers treated with 1 wt% of NaOH treatment has greater potential to be used as reinforcement material in a composite application than IB fibers. In addition, OB fibers constitute a larger weight fraction of the stem than IB fibers. However, future studies may be conducted to investigate the behavior of these treated

fibers in a composite application, and separation of IB fiber from OB fiber may not have a significant effect on properties to justify the added cost of material preparation.

ACKNOWLEDGMENTS

The corresponding author is thankful to the Ministry of Education of Malaysia and Universiti Putra Malaysia for the graduate program sponsorships, and Dr. Muszynski and Milo Clauson for assisting in setting up the DIC system. The authors are also grateful to Dirk Wallace for supplying the grape cane material for this project.

REFERENCES

Ab Ghani AF (2016) Digital image correlation technique in measuring deformation and failure of composite and adhesive. J Eng Appl Sci (Asian Res Publ Netw) 11: 13193-13202.

Abdal-hay A, Suardana NPG, Jung DY, Choi KW, Lim JK (2012) Effect of diameters and alkali treatment on the tensile properties of date palm fiber reinforced epoxy composites. Int J Precis Eng Manuf 13:1199-1206.

Alma MH, Basturk MA (2006) Liquefaction of grapevine cane (*Vitis vinisera* L.) waste and its application to phenol–formaldehyde type adhesive. Ind Crops Prod 24:171-176.

Alves Fidelis ME, Pereira TVC, Gomes O da FM, Silva FA, Filhoa RDT (2013) The effect of fiber morphology on the tensile strength of natural fibers. J Mater Res Technol 2: 149-157.

Aruan Efendy MG, Pickering KL (2014) Comparison of harakeke with hemp fibre as a potential reinforcement in composites. Compos Part A Appl Sci Manuf 67:259-267.

ASTM C1557-14 (2014) Standard test method for tensile strength and Young's modulus of fibers. America Society for Testing Materials ASTM, West Conshohocken, PA.

Bakar BFA, Kamke FA (2020) Comparison of alkali treatments on selected chemical, physical and mechanical properties of grape cane fibers. Cellulose 27(13):7371-7387.

Biswas S, Ahsan Q, Cenna A, Hasan M, Hasan M (2013) Physical and mechanical properties of jute, bamboo and coir natural fiber. Fibers Polym 14:1762-1767.

Burnard MD, Muszyński L, Leavengood S, Ganio L (2019) Correction to: An optical method for rapid examination of check development in decorative plywood panels. Eur J Wood Wood Prod 77:171-171.

Cai M, Takagi H, Nakagaito AN, Lia Y, Waterhouse GIN (2016) Effect of alkali treatment on interfacial bonding in abaca fiber-reinforced composites. Compos Part A Appl Sci Manuf 90:589-597.

Cerbu C, Xu D, Wang H, Roşca IC (2018) The use of digital image correlation in determining the mechanical properties of materials. IOP Conf Ser Mater Sci Eng 399:012007.

Defoirdt N, Biswas S, Vriese LD, Tran LQN, Acker JV, Ahsan Q, Gorbatikh L, Vuure AV, Verpoest I (2010) Assessment of the tensile properties of coir, bamboo and jute fibre. Compos Part A Appl Sci Manuf 41:588-595.

Depuydt D, Hendrickx K, Biesmans W, Ivens J, Vuure AWV (2017) Digital image correlation as a strain measurement technique for fibre tensile tests. Compos Part A Appl Sci Manuf 99:76-83.

Fiore V, Scalici T, Nicoletti F, Vitale G, Prestipino M, Valenza A (2016) A new eco-friendly chemical treatment of natural fibres: Effect of sodium bicarbonate on properties of sisal fibre and its epoxy composites. Compos Part B Eng 85:150-160.

Goudenhooft C, Siniscalco D, Arnould O, Bourmaud A, Sire O, Gorshkova T, Baley C (2018) Investigation of the mechanical properties of flax cell walls during plant development: The relation between performance and cell wall structure. Fibers (Basel) 6:1-9.

Huang Y, Fei B (2017) Comparison of the mechanical characteristics of fibers and cell walls from moso bamboo and wood. BioResources 12:8230-8239.

Ilankeeran PK, Mohite PM, Kamle S (2012) Axial tensile testing of single fibres. Mod Mech Eng 2:151-156.

Mancera C, Mansouri N-EE, Ferrando F, Salvado J (2011) The suitability of steam exploded *Vitis vinifera* and alkaline lignin for the manufacture of fiberboard. BioResources 6:4439-4453.

Martin N, Mouret N, Davies P, Baley C (2013) Influence of the degree of retting of flax fibers on the tensile properties of single fibers and short fiber/polypropylene composites. Ind Crops Prod 49:755-767.

Oushabi A, Sair S, Oudrhiri Hassani F, Abbouda Y, Tananea O, El Bouari A (2017) The effect of alkali treatment on mechanical, morphological and thermal properties of date palm fibers (DPFs): Study of the interface of DPF–Polyurethane composite. S Afr J Chem Eng 23:116-123.

Pereira H (2007) The chemical composition of cork. Pages 55-99 *in* Pereira H (ed.), *Cork: Biology, Production and Uses*. United Kingdom: Elsevier.

Placet V, Trivaudey F, Cisse O, Gucheret-Retel V, Boubakar ML (2012) Diameter dependence of the apparent tensile modulus of hemp fibres: A morphological, structural or ultrastructural effect? Compos Part A Appl Sci Manuf 43: 275-287.

Rajeshkumar G, Hariharan V, Scalici T (2016) Effect of NaOH treatment on properties of *Phoenix* sp. fiber. J Nat Fibers 13:702-713.

Schwarzkopf M, Muszyński L, Hammerquist CC, Nairn JA (2017) Micromechanics of the internal bond in wood plastic composites: Integrating measurement and modeling. Wood Sci Technol 51:997-1014.

Shah DU (2013) Developing plant fibre composites for structural applications by optimising composite parameters: A critical review. J Mater Sci 48:6083-6107.

Shah DU, Reynolds TP, Ramage MH (2017) The strength of plants: Theory and experimental methods to measure the mechanical properties of stems. J Exp Bot 68:4497-4516.

Shahzad A (2013) A study in physical and mechanical properties of hemp fibres. Adv Mater Sci Eng 2013:1-9.

Silva FDA, Chawla N, de Toledo Filhoa RD (2008) Tensile behavior of high performance natural (sisal) fibers. Compos Sci Technol 68:3438-3443.

Spinelli R, Nati C, Pari L, Mescalchin E, Magagnotti N (2012) Production and quality of biomass fuels from mechanized collection and processing of vineyard pruning residues. Appl Energy 89:374-379.

Tomczak F, Sydenstricker THD, Satyanarayana KG (2007) Studies on lignocellulosic fibers of Brazil. Part II: Morphology and properties of Brazilian coconut fibers. Compos Part A Appl Sci Manuf 38:1710-1721.

Toscano G, Alfano V, Scarfone A, Pari L (2018) Pelleting vineyard pruning at low cost with a mobile technology. Energies 11:2477.

Valášek P, Müller M, Šleger V (2017) Influence of plasma treatment on mechanical properties of cellulose-based fibres and their interfacial interaction in composite systems. BioResources 12:5449-5461.

Wine Institute (2014) World vineyard acreage by country 2014. Trade Data and Analysis. https://www.wineinstitute.org/resources/statistics.

Yeniocak M, Göktaş O, Erdil YZ, Özen E, Mehmet A (2014) Investigating the use of vine pruning stalks (*Vitis vinifera* L. cv. Sultani) as raw material for particleboard manufacturing. Wood Res 59:167-176.

Yzombard A, Gordon SG, Miao M (2014) Morphology and tensile properties of bast fibers extracted from cotton stalks. Textile Res J 84:303-311.

Zeng X, Mooney SJ, Sturrock CJ (2015) Assessing the effect of fibre extraction processes on the strength of flax fibre reinforcement. Compos Part A Appl Sci Manuf 70:1-7.

Zhang H, Li Z, Yang S, Zhang W, Sun Y, Chen S, Luo C (2019) Comparison of some key parameters contributing to lignocellulosic fiber deformation behavior by a mathematical model. Bioresources 14:4136-4145.

Zhao J, Zhao D (2013) Investigation of strain measurements using digital image correlation with a finite element method. J Opt Soc Korea 17:399-404.